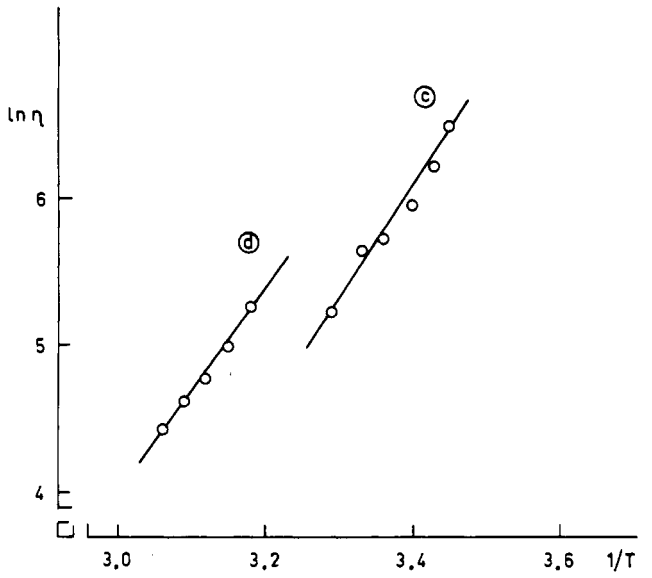

Figure 1. ln η vs. $1/T$: (c) $LiNO_3$ (1)–CH_3CONH_2 (2); (d) $Ca(NO_3)_2$ (1)–CH_3CONH_2 (2).

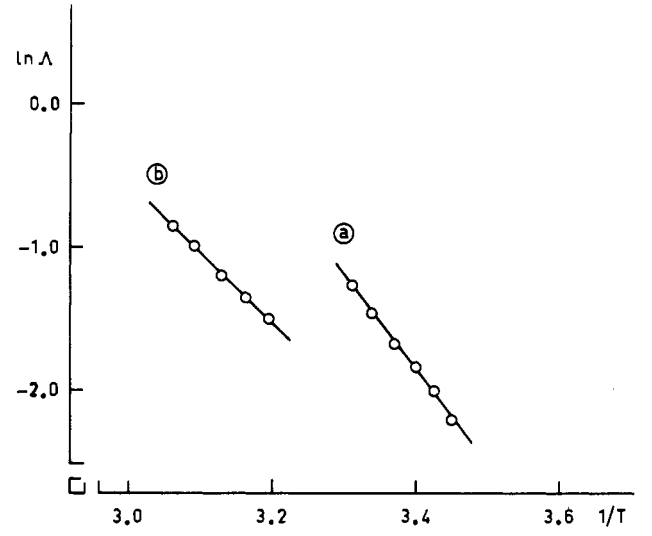

Figure 2. ln Λ vs. $1/T$: (a) $LiNO_3$ (1)–CH_3CONH_2 (2); (b) $Ca(NO_3)_2$ (1)–CH_3CONH_2 (2).

These solutions, as pointed out previously (*3*), present a complex behavior that, following cryoscopic and ultrasonic investigations (*3*–*6*), may be explained on the basis of aggregation phenomena of solvated ions. The conductivity is higher for Ca^{2+} solutions and this fact is in line with the higher charge of this ion. The viscosity of Ca^{2+} solutions is higher and is probably due to the following mechanism of equilibria:

$$MX \rightleftarrows M^+ + X^-$$

$$M^+ + xS \rightleftarrows MS_x^+$$

$$X^- + yS \rightleftarrows XS_y^-$$

$$MS_x^+ + XS_y^- + nS \rightleftarrows \text{aggregate}$$

The fact that the viscosity of Ca^{2+} solutions is higher than Li^+ solutions means that the aggregates in Ca^{2+} solutions are more extended in comparison with aggregates in Li^+ solutions.

The slope in the Arrhenius plots must be regarded as a temperature coefficient and not as a true E_{act}/R, owing to equilibria involved in these solutions.

The fact that the temperature coefficient of the equivalent conductivity is higher for Ca^{2+} solutions may also be explained in terms of the suggested equilibria; i.e., the temperature increase affects the equilibrium aggregates and the resulting free ions increase the conductivity.

The temperature coefficient of viscosity is higher for Li^+ solutions and this experimental evidence may be explained with the following argument: the aggregates with Li^+ ions are less stable than the aggregates with Ca^{2+} ions, also borne out by our cryoscopic measurements.

Acknowledgment

We thank L. Amici for technical assistance.

Glossary

η	viscosity, cP
Λ	equivalent conductivity
χ	specific electrical conductivity, Ω^{-1} cm^{-1}

Registry No. $LiNO_3$, 7790-69-4; $Ca(NO_3)_2$, 10124-37-5.

Literature Cited

(1) Castellani, F.; Berchiesi, G.; Pucciarelli, F.; Bartocci, V. *J. Chem. Eng. Data* **1981**, *26*, 150.
(2) Castellani, F.; Berchiesi, G.; Pucciarelli, F.; Bartocci, V. *J. Chem. Eng. Data* **1982**, *27*, 45.
(3) Berchiesi, G.; Giola Lobbia, G.; Bartocci, V.; Vitali, G. *Thermichim. Acta* **1983**, *70*, 317.
(4) Berchiesi, G.; Vitali, G.; Passamonti, P.; Plowiec, R. *J. Chem. Soc., Faraday Trans. 2* **1983**, *79*, 1257.
(5) Berchiesi, G.; Castellani, F.; Pucciarelli, F. *J. Pure Appl. Ultrason.* **1983**, *5*, 66.
(6) Plowiec, R.; Amico, A.; Berchiesi, G. *J. Chem. Soc., Faraday Trans. 2*, in press.
(7) Harned, H. S.; Owen, B. B. "The Physical Chemistry of Electrolytic Solutions", 3rd ed.; Reinhold: New York, 1958; p 197.
(8) Berchiesi, G.; Leonesi, D.; Cingolani, A. *J. Therm. Anal.* **1978**, *9*, 171.

Received for review April 25, 1984. Accepted October 2, 1984. Thanks are due to Ministero della Pubblica Istruzione (Rome) for financial support.

Vapor–Liquid Equilibria of the System Trimethyl Borate (1)–*n*-Heptane (2)

David Scott Niswonger, Charles A. Plank,* and Walden L. S. Laukhuf

Department of Chemical and Environmental Engineering, University of Louisville, Louisville, Kentucky 40292

Vapor–liquid equilibria for the binary system trimethyl borate (1)–*n*-heptane (2) have been measured at 101 325 Pa. Data have been checked for thermodynamic consistency and also correlated by Wilson equations.

The isobaric vapor–liquid equilibria of the trimethyl borate (1)–*n*-heptane (2) system were measured at 101 325 ± 133 Pa (760 ± 1 torr). An Altsheler still (circulation type) was used and is described in detail by Hala et al. (*1*). The present version incorporates two thermocouples, one near the surface of the

0021-9568/85/1730-0209$01.50/0

Table I. Physical Properties of the Pure Components

component	density at 298.15 K, kg/m³ measd	density at 298.15 K, kg/m³ lit.	refractive index at 298.15 K measd	refractive index at 298.15 K lit.	bp, K measd	bp, K lit.
trimethyl borate	927.5	927.3 (2)	1.355 03	1.355 0 (3)	341.85 ± 0.1	341.85 (4)
n-heptane	679.5	679.51 (5)	1.387 55[a]	1.387 60 (5)[a]	371.65 ± 0.1	371.56 (5)

vapor pressure of trimethyl borate, $\ln P^0 = 13.1756 - 1357.14/(T - 134.33)$, ref 6
vapor pressure of *n*-heptane, $\ln P^0 = 15.8737 - 2911.32/(T - 56.51)$, ref 7

[a] Refractive index for *n*-heptane reported at 293.15 K.

Table II. Experimental Results

[borate], mole fraction liquid	[borate], mole fraction vapor	T, K	activity coeff γ_1	activity coeff γ_2
0.000	0.000	371.6		1.000
0.016	0.044	370.5	1.264	1.001
0.048	0.122	368.8	1.227	0.999
0.106	0.255	365.2	1.281	1.002
0.148	0.317	363.2	1.206	1.021
0.181	0.396	361.1	1.278	1.010
0.241	0.454	359.3	1.155	1.033
0.284	0.509	357.6	1.148	1.036
0.354	0.586	355.1	1.133	1.050
0.410	0.634	353.2	1.114	1.077
0.470	0.689	351.5	1.104	1.076
0.533	0.736	349.6	1.097	1.103
0.636	0.801	347.7	1.057	1.196
0.762	0.870	345.1	1.034	1.238
0.834	0.909	343.8	1.027	1.297
0.911	0.957	342.6	1.023	1.208
0.948	0.977	341.9	1.024	1.120
1.000	1.000	341.9	1.000	

boiling liquid and one in the vapor space directly above the liquid level. These two thermocouples were both calibrated and in general gave the same value during operation. When they differed, the liquid temperature was reported. Temperatures are believed to be accurate to ±0.1 K.

Materials Used

The trimethyl borate was manufactured by Aldrich Chemical Co. Inc. and was received at 98% nominal purity. Successive simple distillations were performed on this material using the "heart cuts" and recovering approximately 40% of the original material. The *n*-heptane was manufactured by Burdick and Jackson Inc., reported to be of greater than 99.9% purity, and was used as received. Properties of these materials compared with literature data are shown in Table I.

Method of Analysis

Analysis was made by using refractive index measurements along with a carefully prepared calibration curve. Measurements were made at 293.15 K by using a Bausch and Lomb refractometer along with a light source employing the sodium D line (λ = 5893 Å). The instrument is capable of providing a precision of ±0.000 03 refractive index unit. The temperature of the prism was controlled to ±0.1 K.

Discussion of Results

The experimental results are shown in Table II and Figure 1. Data show the system to be slightly nonideal with activity coefficients between 1.0 and 1.28. Activity coefficients were calculated from the equation

$$\gamma_i = y_i \Pi / \Phi x_i P^0$$

where $\Phi = \phi_i/\hat{\phi}_i$, the ratio of the fugacity coefficient of the pure component at its vapor pressure to the component in the vapor mixture at the total pressure. Fugacity coefficients were calculated by using the Redlich and Kwong equation. Values of Φ ranged from 0.98 to 1.03. The data were subjected to

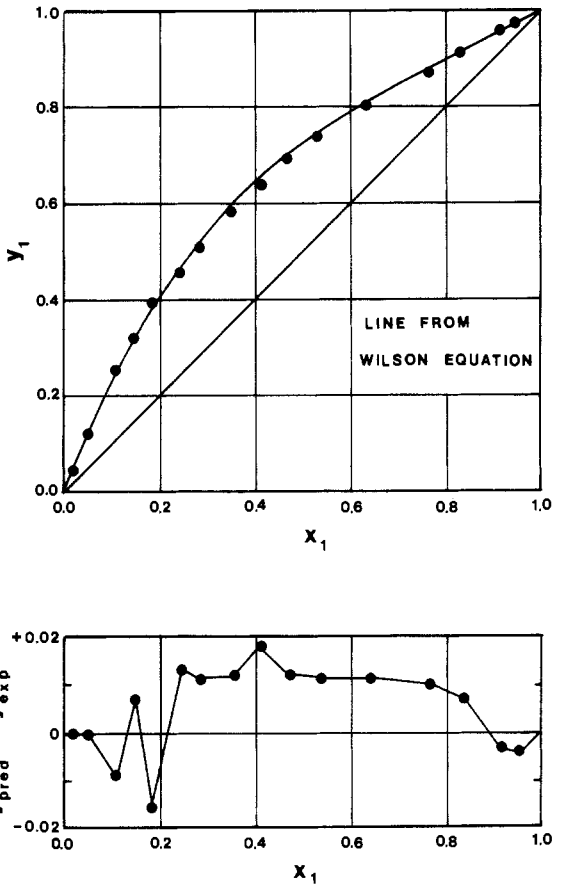

Figure 1. Trimethyl borate (1)–*n*-heptane (2).

a thermodynamic consistency test as suggested by Fredenslund et al. (8). In this procedure the excess Gibbs function is calculated from the experimental temperature, liquid compositions, and activity coefficients. The resulting G^E/RT vs. x data are fitted by Legendre polynomials (third order in the present work) and activity coefficients then determined by making use of the partial molal relationship to the excess function. Values of y_i are then estimated and compared with measured values. For this work the average deviation between measured and estimated vapor concentrations was 0.013 mole fraction.

The data were also compared with the Van Laar, Margules, and Wilson models (9). Data were best fitted by the Wilson equation with parameters $G_{12} = 1.4252$ and $G_{21} = 0.4589$. The average error in vapor-phase compositions by this model was slightly less than 0.01 mole fraction. The line in Figure 1 represents this Wilson model and the lower part of the figure shows the deviation of each point.

Glossary

G^E	excess Gibbs function
G_{ij}	binary parameter for Wilson equations
P^0	vapor pressure, mmHg
R	gas constant
T	temperature, K

x liquid-phase concentration, mole fraction
y vapor-phase concentration, mole fraction

Greek Letters

γ_i activity coefficient
Π total pressure, mmHg
Φ ratio of fugacity coefficients
$\hat{\phi}_i$ fugacity coefficient in vapor mixture at Π
ϕ_i fugacity coefficient of pure component at P^0

Registry No. Trimethyl borate, 121-43-7; heptane, 142-82-5.

Literature Cited

(1) Hala, E.; Pick, J.; Fried, V.; Vilim, O. "Vapor-Liquid Equilibrium", 2nd English ed.; Pergamon Press: Oxford, 1967; pp 305-6.
(2) Christopher, P. M.; Washington, H. W. *J. Chem. Eng. Data* **1969**, *14*, 437.
(3) Munster, N.; Plank, C. A.; Laukhuf, W. L. S.; Christopher, P. M. *J. Chem. Eng. Data* **1984**, *29*, 178.
(4) Lange, N. A. "Handbook of Chemistry", 11th ed.; Handbook Publishing: Sandusky, OH, 1973.
(5) "High Purity Solvent Guide"; Physical Property Section, Burdick and Jackson Laboratories, Inc.: Muskegon, MI, 1980.
(6) Plank, C. A.; Christopher, P. M. *J. Chem. Eng. Data* **1976**, *21*, 211.
(7) Reid, R. C.; Prausnitz, J. M.; Sherwood, T. K. "The Properties of Gases and Liquids", 3rd ed.; McGraw-Hill: New York, 1977; p 432.
(8) Fredenslund, A.; Gmehling, J.; Rasmuessen, P. "Vapor-Liquid Equilibria Using UNIFAC"; Elsevier: Amsterdam, 1977.
(9) Smith, J. M.; Van Ness, H. C. "Introduction to Chemical Engineering Thermodynamics", 3rd ed.; McGraw-Hill: New York, 1975.

Received for review May 9, 1984. Accepted August 27, 1984.

Sound Velocity and Electrolytic Conductivity in the Molten Sodium Nitrite–Potassium Nitrate System

Shinya Okuyama, Katsusaburo Toyoda,† Ryuzo Takagi, and Kazutaka Kawamura*

Research Laboratory for Nuclear Reactors, Tokyo Institute of Technology, Meguro-ku, Tokyo 152, Japan

Sound velocity and electrolytic conductivity in binary molten salt mixtures of $NaNO_2$–KNO_3, which is a candidate for heat reservoir material, were determined by an ultrasonic pulse–echo method and a direct current (dc) method, respectively. The adiabatic and isothermal compressibilities, the isochoric specific heat, and the molar conductivity were derived with available data on isobaric specific heat and density. The concentration dependences of these properties show significant deviation from linearity.

Introduction

Mixtures of $NaNO_2$ and KNO_3 have as low a melting point as HTS (heat transfer salt; $NaNO_2$–KNO_3–$NaNO_3$ 49/44/7 mol %) and are therefore promising candidates as heat reservoir materials (*1*). It is useful to know the concentration dependence of properties of the mixture, since a concentration distribution appears in a phenomenon with mass transfer, e.g., corrosion. In this work the sound velocity and the electrolytic conductivity in this mixture have been measured. The sound velocity was measured by an ultrasonic pulse–echo method. The sound velocity gives us some thermodynamic properties, such as adiabatic and isothermal compressibilities, and isochoric specific heat with available data on density and isobaric specific heat. The molar conductivity is derived from the electrolytic conductivity, which was measured by a dc method, and available density data. A dc method in contrast to an ac method produces no polarization impedance (*2*).

The sound velocity (*3*) and the electrolytic conductivity (*4*) of HTS were reported previously. They will be compared with the corresponding quantities obtained in this work.

Experimental Section

Chemicals. The salts $NaNO_2$ and KNO_3 used were of analytical reagent grade (Wako Chemicals). They were melted and then dispersed with N_2 gas. Additionally they were passed through a glass filter just before experimental run. The content of $NaNO_2$, which is reported to be thermally unstable at higher temperatures, was checked before and after each run. The experimental data were accepted when the following relation was satisfied within experimental error:

$$N_{Na}M_{NaNO_2} + N_KM_{KNO_3} = W \quad (1)$$

In eq 1 W is the weight of the mixture sampled from the melt, N_X is the molar quantity of a component cation X, and M_Y is the formula weight of a component salt Y. The quantities N_{Na} and N_K were determined by flame spectrophotometry. Relative error in N_{Na} and N_K was estimated to be ±2%. During each experimental run the sample melts were kept under N_2 gas atmosphere to depress the decomposition of $NaNO_2$ (*5*).

Sound Velocity Experiment. Figure 1 shows a schematic diagram of the apparatus, which is equipped with three micrometers (b). Except for this modification the apparatus is similar to that employed previously (*3*). These micrometers are used to adjust parallelism between planes of the quartz conductivity rod (f) and the bottom of the cell (j). The experimental procedure was described in detail previously (*3*).

Electrolytic Conductivity Experiment. The experimental equipment and technique are similar to those used by King and Duke (*6*). The cell constant was 14.90 cm^{-1}, which was de-

Table I. Sound Velocity in Molten $NaNO_2$–KNO_3 System

U (m s^{-1}) = $a + bT + cT^2$

run no.	p_{NaNO_2}[a]	$10^{-3}a$	b	10^3c	temp range/K
1	1.000	3.0631	−2.8395	1.3679	571–689
2	0.811	3.2057	−3.3968	1.8228	511–666
3	0.653	2.7257	−1.7523	0.3649	437–649
4	0.491	2.7572	−1.9526	0.5597	444–686
5	0.317	2.9514	−2.6471	1.1114	483–700
6	0.182	3.4120	−3.9913	2.0897	546–681
7	0.000	2.4910	−1.1262	−0.1153	617–747

ref	salts	$10^{-3}a$	b	10^3c	temp range/K
3	$NaNO_2$	2.7061	−1.470		565–586
3	KNO_3	2.4807	−1.187		625–713
7	KNO_3	2.483	−1.194		593–803
8	KNO_3	2.450	−1.12		609–712
9	KNO_3	2.7663	−1.9149	0.4686	*b*

[a] Mole fraction of $NaNO_2$. [b] Unspecified in the literature.

† Shibaura Institute of Technology, Shibaura, Minato-ku, Tokyo 108, Japan.

0021-9568/85/1730-0211$01.50/0